

Strain induced tunable anisotropic magnetoresistance in $\text{La}_{0.67}\text{Ca}_{0.33}\text{MnO}_3/\text{BaTiO}_3$ heterostructures

Yali Xie, Huali Yang, Yiwei Liu, Zhihuan Yang, Bin Chen, Zhenghu Zuo, Sadhana Katlakunta, Qingfeng Zhan, and Run-Wei Li

Citation: *Journal of Applied Physics* **113**, 17C716 (2013); doi: 10.1063/1.4795841

View online: <http://dx.doi.org/10.1063/1.4795841>

View Table of Contents: <http://scitation.aip.org/content/aip/journal/jap/113/17?ver=pdfcov>

Published by the [AIP Publishing](#)

Articles you may be interested in

[Anisotropic resistivities in anisotropic-strain-controlled phase-separated \$\text{La}_{0.67}\text{Ca}_{0.33}\text{MnO}_3/\text{NdGaO}_3\(100\)\$ films](#)
Appl. Phys. Lett. **103**, 072407 (2013); 10.1063/1.4818636

[Anisotropic magnetoresistance in epitaxial \$\text{La}_{0.67}\(\text{Ca}_{1-x}\text{Sr}_x\)\text{MnO}_3\$ films](#)
J. Appl. Phys. **113**, 17C722 (2013); 10.1063/1.4798798

[Structure and magnetotransport properties of epitaxial nanocomposite \$\text{La}_{0.67}\text{Ca}_{0.33}\text{MnO}_3:\text{SrTiO}_3\$ thin films grown by a chemical solution approach](#)
Appl. Phys. Lett. **100**, 082403 (2012); 10.1063/1.3688048

[Phase evolution and the multiple metal-insulator transitions in epitaxially shear-strained \$\text{La}_{0.67}\text{Ca}_{0.33}\text{MnO}_3/\text{NdGaO}_3\(001\)\$ films](#)
J. Appl. Phys. **108**, 083912 (2010); 10.1063/1.3499650

[Temperature dependence of magnetoresistance and nonlinear conductance of the bicrystal grain boundary in epitaxial \$\text{La}_{0.67}\text{Ba}_{0.33}\text{MnO}_3\$ thin films](#)
Appl. Phys. Lett. **81**, 325 (2002); 10.1063/1.1481785

The logo for AIP APL Photonics is displayed. It features the letters 'AIP' in a large, white, sans-serif font on the left, followed by a vertical line and the words 'APL Photonics' in a smaller, white, sans-serif font on the right. The background is a dark red with a bright yellow sunburst effect in the upper right corner.

APL Photonics is pleased to announce
Benjamin Eggleton as its Editor-in-Chief



Strain induced tunable anisotropic magnetoresistance in $\text{La}_{0.67}\text{Ca}_{0.33}\text{MnO}_3/\text{BaTiO}_3$ heterostructures

Yali Xie,^{1,2} Huali Yang,^{1,2} Yiwei Liu,^{1,2} Zhihuan Yang,^{1,2} Bin Chen,^{1,2} Zhenghu Zuo,^{1,2} Sadhana Katlakunta,^{1,2} Qingfeng Zhan,^{1,2,a)} and Run-Wei Li^{1,2,a)}

¹Key Laboratory of Magnetic Materials and Devices, Ningbo Institute of Material Technology and Engineering, Chinese Academy of Sciences, Ningbo 315201, People's Republic of China

²Zhejiang Province Key Laboratory of Magnetic Materials and Application Technology, Ningbo Institute of Material Technology and Engineering, Chinese Academy of Sciences, Ningbo 315201, People's Republic of China

(Presented 17 January 2013; received 1 November 2012; accepted 14 December 2012; published online 25 March 2013)

In this paper, we investigated the influence of strain on anisotropic magnetoresistance (AMR) in $\text{La}_{0.67}\text{Ca}_{0.33}\text{MnO}_3$ (LCMO) films epitaxially grown on $\text{BaTiO}_3(001)$. For 250-nm-thick LCMO film, the AMR shows a peak near the metal-insulator transition (MIT) temperature, which is similar to that in bulk LCMO. When the thickness of LCMO is decreased to 150 nm, the AMR value achieves a maximum at low temperature. For 80-nm-thick LCMO film, in addition to the appearance of the maximum AMR at low temperature, the symmetry and sign of AMR are also changed, associated with interface strain in the different phases of BaTiO_3 . In comparison, the AMR for the reference LCMO films grown on $\text{SrTiO}_3(001)$ shows a maximum value near the MIT temperature regardless of the thickness of film. Our experiment results suggest that not only the strain value but also the distortion type can considerably tune the AMR of LCMO films. © 2013 American Institute of Physics. [<http://dx.doi.org/10.1063/1.4795841>]

Anisotropic magnetoresistance (AMR) effect has attracted much interest for decades due to their applications in data storages and magnetic sensors.^{1–5} Recently, an anomalously large AMR has been found in $\text{La}_{0.67}\text{Ca}_{0.33}\text{MnO}_3$ (LCMO) single crystal, polycrystalline, and thin films,^{6–9} which is caused by the magnetic field tunable metal-insulator transition (MIT). Previous works indicated that the unusual AMR in epitaxial manganite films^{9–11} depends on the lattice constant,¹² film thickness,¹³ crystalline direction,^{14,15} and state of strain.^{16,17} Therefore, to control and tune the AMR of perovskite manganites for the potential applications, the effect of mechanical strain on the AMR needs to be known in detail. Technologically, for epitaxial thin films, the variables such as lattice relaxation, stoichiometry, crystalline quality, and microstructure, which strongly affect the strain status produced by the lattice mismatch between the films and the substrates, are very difficult to be reproduced in different samples.¹⁸ Therefore, it is hard to discriminate the different strain states from sample to sample and systematically study the effect of strain on AMR of perovskite manganite films. On the other hand, BaTiO_3 (BTO) single crystal possesses rich structural transitions taken placed at different temperatures, for example, the rhombohedra to orthorhombic structural phase transition occurring at 183 K and the orthorhombic to tetragonal structural phase transition at 278 K.¹⁹ The structural phase transitions of BTO can serve as the strain source for films grown on BTO single crystals. In this way, by changing temperature, the different strain states can be easily achieved in magnetic films. In the present investigation, LCMO thin films were epitaxially

grown on BTO single crystal substrate and the effect of strain produced by the structural phase transitions of BTO substrate at different temperatures on AMR behaviors of LCMO thin films was studied. The LCMO films grown on STO substrates were chosen as the reference samples because STO possesses no structural phase transition in the range of our measurement temperature. The unusual AMR effect was observed under various magnetic fields and temperatures for LCMO/BTO thin films, which suggests that not only the strength but also the type of strains could considerably change the AMR behavior of LCMO films.

Different thicknesses of LCMO films were epitaxially grown on both $\text{BTO}(001)$ and $\text{STO}(001)$ substrates by using pulsed laser deposition (PLD) method, and the corresponding lattice mismatches between films and substrates are 2% and 1.7%, respectively. All the LCMO films are in a single phase with a perovskite structure as confirmed by X-ray diffraction (XRD). The angular dependence of magnetoresistance was measured by means of a Physical Property Measurement System (PPMS, Quantum Design). The geometries of the magnetic field (H) rotating in the yz plane and the current (I) applied in the experiments are shown in the inset of Fig. 1. θ is the angle between the field and c -axis in the yz plane. During the measurements, H was kept perpendicular to the current flow direction in order to minimize the ordinary magnetoresistance caused by the Lorentz force acting on the conduction electrons, and the resistance was measured as a function of the angle (θ) at different temperatures. The AMR amplitude is defined as the maximum of $[R(\theta) - R(0)]/R(0)$, where $R(\theta)$ and $R(0)$ are the resistance for the magnetic field orientations at angles of θ and 0, respectively.

The temperature dependence of resistance for the LCMO/BTO with different thicknesses is shown in Fig. 1. For the

^{a)}Authors to whom correspondence should be addressed. Electronic addresses: zhanqf@nimte.ac.cn and runweili@nimte.ac.cn.

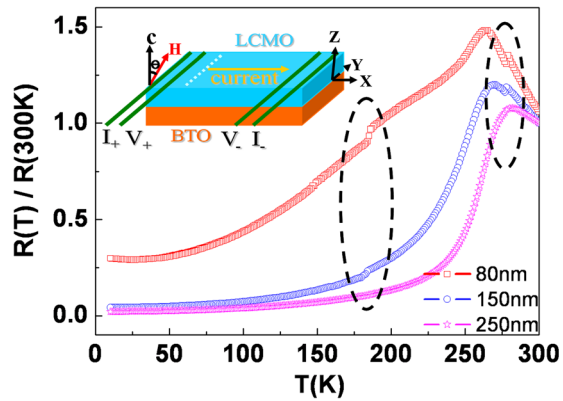


FIG. 1. Temperature dependence of resistance for the LCMO/BTO films with different thicknesses. The inset shows a schematic arrangement for the measurements of the samples.

250-nm-thick LCMO film, the temperature dependent resistance shows a maximum at the MIT temperature of 280 K, which is in good agreement with LCMO single crystal. However, for the 150-nm-thick sample, in addition to the peak at the MIT temperature of 270 K, two sudden drops of resistance are observed at 190 and 275 K. For the 80-nm-thick LCMO film, the R-T curve shows a maximum at the MIT temperature of 263 K and two much significant drops at 190 and 275 K. These two temperatures where the resistance drops occur coincide well with the structural phase transition temperatures of BTO. Therefore, the resistances drop at these temperatures in LCMO/BTO films can be attributed to the mechanical strain which is caused by the phase transitions of BTO. Moreover, compared with the thicker films, the 80-nm-thick LCMO film exhibits an R-T curve with much slow slopes, indicating that the temperature for the occurrence of

phase separation, i.e., the coexistence of paramagnetic and ferromagnetic phases, is broadened from the MIT temperature to the low temperature. Our experimental observations demonstrate that the strain which comes from the BTO phase transition can greatly change the transport properties of LCMO films, and the strain-transfer effect shows more effective in thinner LCMO films.

Figure 2 shows the AMR behaviors of LCMO/BTO and LCMO/STO heterostructures at different temperatures with the magnetic field fixed at 5 kOe. The AMR of LCMO/BTO film with 250 nm in thickness reaches a maximum value of about 6% at 265 K, as shown in Fig. 2(a), which is close to the MIT temperature of 280 K. The AMR curves show the $\cos^2 \theta$ behavior regardless of the measuring temperatures. Currently, the mechanism for AMR measured in our current geometry has not yet been fully understood. As reported in our previous work,⁶ the anomalously large AMR observed in LCMO single crystal is likely due to the dissimilar response of Jahn-Teller lattice distortions to external magnetic field, thus, creating distinct effects on the transport properties through different couplings with the double-exchange interaction. For the 150-nm-thick LCMO/BTO film, the AMR value is decreased with increasing temperature and a maximum is found at 10 K, as shown in Fig. 2(b). The AMR is negative in the range of our measuring temperatures from 10 to 300 K. The AMR curves show an oval shape at low temperature of 10 K, but gradually change to the $\cos^2 \theta$ behavior with increasing temperature. For the 80-nm-thick LCMO film, as shown in Fig. 2(c), the AMR value achieves a maximum of 6.6% at 10 K. With increasing temperature, the AMR value is reduced and the sign is changed from negative to positive at the temperature of 265 K. Meanwhile, the symmetry of AMR is changed from twofold to fourfold at 250 K.

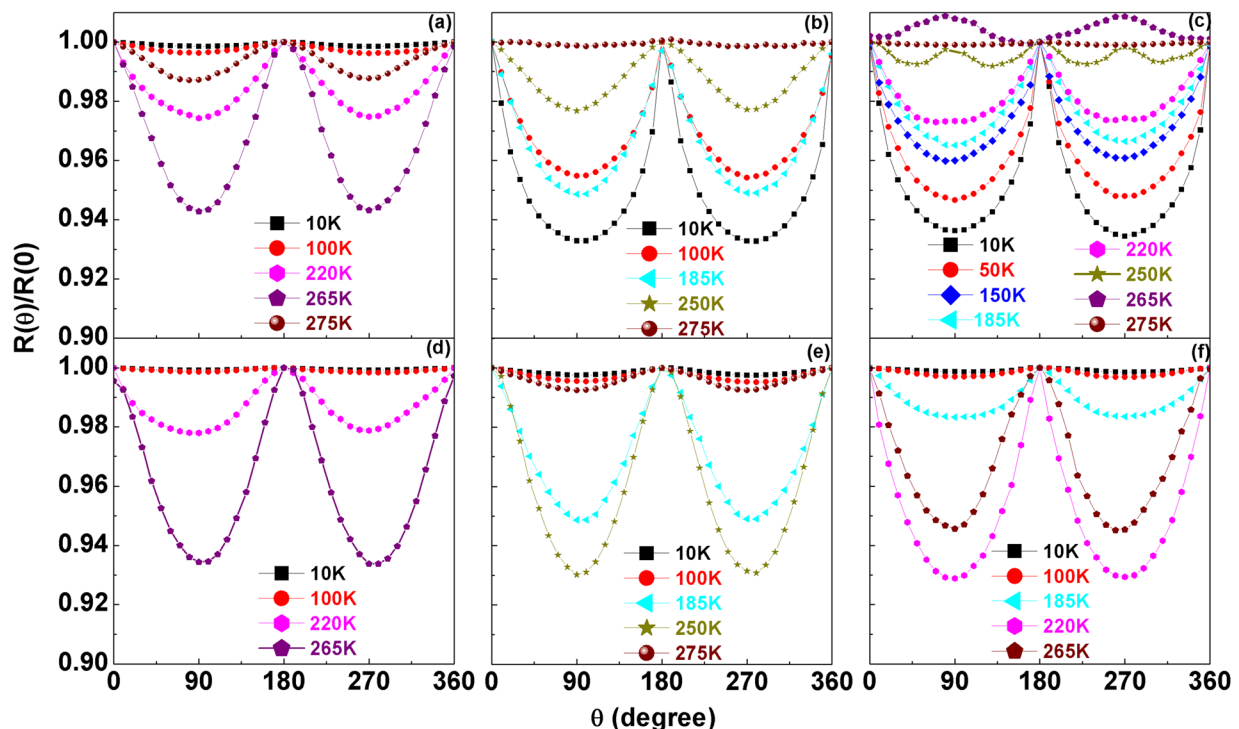


FIG. 2. The normalized angular dependence of resistance measured at different temperatures with $H = 5$ kOe for LCMO/BTO films with the thicknesses of (a) 250 nm, (b) 150 nm, and (c) 80 nm, and for LCMO/STO films with the thicknesses of (d) 250 nm, (e) 150 nm, and (f) 80 nm.

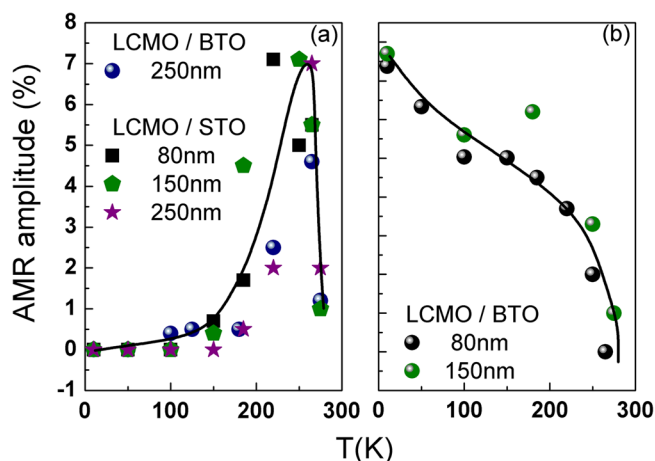


FIG. 3. (a) The temperature dependence of AMR for the LCMO/BTO and LCMO/STO films with different thicknesses. (b) The temperature dependence of AMR for the LCMO/BTO films with different thicknesses.

With further elevating the temperature, the fourfold symmetric AMR behavior disappears. It should be noted that this fourfold symmetric AMR cannot be fitted by two twofold symmetries. At high temperature above the MIT temperature, the AMR behavior finally disappears. Due to the more significant strain effect in thinner films, the changes in AMR value, symmetry, and sign are more clearly seen in the 80-nm-thick LCMO film as compared with that in the 150-nm-thick one. For all LCMO/STO reference samples, the AMR reaches a maximum value at the MIT temperature and shows the $\cos^2\theta$ behavior, which agrees well with that of the LCMO bulk materials, as shown in Figs. 2(d)–2(f).

The drastic differences in AMR behaviors between LCMO/BTO and LCMO/STO samples revealed above obviously arise from the different strain states caused by the substrates of STO and BTO. For the 80-nm-thick LCMO/BTO film, the AMR shows a maximum at low temperature and the change in the symmetry and sign with varying the temperature due to the different strength and type of strains in the different phases of BTO. The strain caused by the BTO rhombohedra phase increases the dissimilar response of Jahn-Teller distortions to external magnetic field in LCMO,^{17,20,21} which gives rise to the maximum AMR occurring at low temperature. The appearance of four-fold symmetric AMR behaviors which is superimposed on the two-fold AMR in the 80-nm-thick LCMO film is ascribed to the strain transferred from the orthorhombic BTO to the LCMO film. With increasing temperature, the strain changes with the expansion of BTO lattice, which leads to the enhancement of four-fold symmetric AMR and the appearance of positive AMR in LCMO films. We therefore conclude that the strain induced by the BTO rhombohedra phase gives rise to the maximum AMR at low temperature, while the strain caused by the BTO orthorhombic phase results in the changes of AMR symmetry and AMR sign. Because the strain-transfer effect is more effective in thinner films, with increasing the thickness of LCMO, although the maximum AMR appears at low temperature for the 150-nm-thick LCMO/BTO film, the changes of AMR sign and symmetry

can be no more observed. For the 250-nm-thick LCMO film, the AMR behavior is very similar to that of the bulk LCMO.

In Fig. 3, we summarized the temperature dependence of AMR ratio for the LCMO/BTO and LCMO/STO heterostructures with different thicknesses. Our result shows that the temperature dependent AMR behaviors strongly depend on both the substrate and the film thickness. The AMR ratio for the 250-nm-thick LCMO/BTO film achieves a maximum at the MIT temperature, which behaves like that of the LCMO bulk materials. The strain effect on AMR behavior is significant for LCMO/BTO films with thickness less than 150 nm. The AMR value is decreased with increasing temperature, which are different from that of LCMO bulk materials. For all the LCMO/STO thin films, the maximum AMR always appears at the MIT temperature. Obviously, the abnormal AMR behaviors observed in LCMO/BTO films originate from the strain effect in the different phases of BTO substrates.

The authors acknowledge the financial support from the National Natural Foundation of China (11274321, 11174302), the State Key Project of Fundamental Research of China (2012CB933004, 2009CB930803), the Chinese Academy of Sciences (CAS), and the Ningbo Science and Technology Innovation Team (2011B82004, 2009B21005), the Projects of Nonprofit Technology & Research in Zhejiang Province (2010C31041), and the Zhejiang and Ningbo Natural Science Foundations.

- ¹H. N. Bertran, *Applied Magnetism* (Kluwer, Dordrecht, 1992).
- ²J. N. Eckstein, I. Bozovic, J. O'Donnell, M. Onellion, and M. S. Rzchowski, *Appl. Phys. Lett.* **69**, 1312 (1996).
- ³M. Ziese and S. P. Sena, *J. Phys.: Condens. Matter* **10**, 2727 (1998).
- ⁴M. Egilmez, M. M. Saber, A. I. Mansour, R. Ma, K. H. Chow, and J. Jung, *Appl. Phys. Lett.* **93**, 182505 (2008).
- ⁵S. Andreev and P. Dimitrova, *J. Optoelectron. Adv. Mater.* **7**, 199 (2005).
- ⁶R. W. Li, H. B. Wang, X. Wang, X. Z. Yu, Y. Matsui, Z. H. Cheng, B. G. Shen, E. W. Plummer, and J. Zhang, *Proc. Natl. Acad. Sci. U.S.A.* **106**, 14224 (2009).
- ⁷W. Ning, Z. Qu, Y. M. Zou, L. S. Ling, L. Zhang, C. Y. Xi, H. F. Du, R. W. Li, and Y. H. Zhang, *Appl. Phys. Lett.* **98**, 212503 (2011).
- ⁸M. Egilmez, R. Ma, K. H. Chow, and J. Jung, *J. Appl. Phys.* **105**, 07D706 (2009).
- ⁹M. Bibes, V. Laukhin, S. Valencia, B. Martinez, J. Fontcuberta, O. Y. Gorbenko, A. R. Kaul, and J. L. Martinez, *J. Phys.: Condens. Matter* **17**, 2733 (2005).
- ¹⁰J. O. Donnell, M. Onellion, M. S. Rzchowski, J. N. Eckstein, and I. Bozovic, *Phys. Rev. B* **54**, R6841 (1996).
- ¹¹J. O. Donnell, J. N. Eckstein, and M. S. Rzchowski, *Appl. Phys. Lett.* **76**, 218 (2000).
- ¹²Q. Li, H. S. Wang, Y. F. Hu, and E. Wertz, *J. Appl. Phys.* **87**, 5573 (2000).
- ¹³M. Egilmez, R. Petterson, K. H. Chow, and J. Jung, *Appl. Phys. Lett.* **90**, 232506 (2007).
- ¹⁴I. C. Infante, V. Laukhin, F. Sanchez, J. Fontcuberta, O. Melnikov, O. Y. Gorbenko, and A. R. Kaul, *J. Appl. Phys.* **99**, 08C502 (2006).
- ¹⁵Y. Z. Chen, J. R. Sun, T. Y. Zhao, J. Wang, Z. H. Wang, B. G. Shen, and N. Pryds, *Appl. Phys. Lett.* **95**, 132506 (2009).
- ¹⁶J. B. Yau, X. Hong, A. Posadas, C. H. Ahn, W. Gao, E. Altman, Y. Bason, L. Klein, M. Sidorov, and Z. Krivokapic, *J. Appl. Phys.* **102**, 103901 (2007).
- ¹⁷L. F. Wang, Z. Huang, X. L. Tan, P. F. Chen, B. W. Zhi, G. M. Li, and W. B. Wu, *Appl. Phys. Lett.* **97**, 242507 (2010).
- ¹⁸M. K. Lee, T. K. Nath, C. B. Eom, M. C. Smoak, and F. Tsui, *Appl. Phys. Lett.* **77**, 3547 (2000).
- ¹⁹H. F. Kay and P. Vousden, *Philos. Mag.* **40**, 1019 (1949).
- ²⁰M. K. Srivastava, A. Kaur, and H. K. Singh, *Appl. Phys. Lett.* **100**, 222408 (2012).
- ²¹F. H. Zhang, Z. Huang, G. Y. Gao, P. F. Chen, L. F. Wang, X. L. Tan, and W. B. Wu, *Appl. Phys. Lett.* **96**, 062507 (2010).